The Plant Cell, Vol. 24: 5058–5073, December 2012, www.plantcell.org

Trafficking of Vacuolar Proteins: The Crucial Role of *Arabidopsis* Vacuolar Protein Sorting 29 in Recycling Vacuolar Sorting Receptor[W]

Hyangju Kang,[a] Soo Youn Kim,[b] Kyungyoung Song,[a] Eun Ju Sohn,[b] Yongjik Lee,[b] Dong Wook Lee,[b] Ikuko Hara-Nishimura,[c] and Inhwan Hwang[a,b,1]

[a] Division of Molecular and Life Sciences, Pohang University of Science and Technology, Pohang 790-784, Korea
[b] Division of Integrative Biosciences and Biotechnology, Pohang University of Science and Technology, Pohang 790-784, Korea
[c] Department of Botany, Graduate School of Science, Kyoto University, Kyoto, 606-8502, Japan

The retromer is involved in recycling lysosomal sorting receptors in mammals. A component of the retromer complex in *Arabidopsis thaliana*, vacuolar protein sorting 29 (VPS29), plays a crucial role in trafficking storage proteins to protein storage vacuoles. However, it is not known whether or how vacuolar sorting receptors (VSRs) are recycled from the prevacuolar compartment (PVC) to the trans-Golgi network (TGN) during trafficking to the lytic vacuole (LV). Here, we report that VPS29 plays an essential role in the trafficking of soluble proteins to the LV from the TGN to the PVC. *maigo1-1* (*mag1-1*) mutants, which harbor a knockdown mutation in *VPS29*, were defective in trafficking of two soluble proteins, *Arabidopsis* aleurain-like protein (AALP):green fluorescent protein (GFP) and sporamin:GFP, to the LV but not in trafficking membrane proteins to the LV or plasma membrane or via the secretory pathway. AALP:GFP and sporamin:GFP in *mag1-1* protoplasts accumulated in the TGN but were also secreted into the medium. In *mag1-1* mutants, VSR1 failed to recycle from the PVC to the TGN; rather, a significant proportion was transported to the LV; VSR1 overexpression rescued this defect. Moreover, endogenous *VSRs* were expressed at higher levels in *mag1-1* plants. Based on these results, we propose that VPS29 plays a crucial role in recycling VSRs from the PVC to the TGN during the trafficking of soluble proteins to the LV.

INTRODUCTION

Plant cells contain two different types of vacuoles with different functions, the lytic vacuole (LV) found in vegetative cells and the protein storage vacuole (PSV) found in seed cells. The LV, which has an acidic pH and occupies 90% of the cellular volume, is involved in the storage of inorganic ions and secondary metabolites; detoxification; the hydrolytic degradation of proteins, lipids, and carbohydrates; and osmotic pressure regulation. By contrast, the PSV has a neutral pH and stores the large amounts of proteins and minerals that are required for germination (Vitale and Raikhel, 1999). In order to function as the LV or PSV, these compartments need a large number of organelle-specific proteins, which are synthesized by endoplasmic reticulum (ER)–associated ribosomes and transported to the ER cotranslationally (Crowley et al., 1994; Rapoport et al., 1996). Subsequently, vacuolar proteins are transported from the ER to the vacuole through the trans-Golgi network (TGN) and the prevacuolar compartment (PVC) (Jürgens, 2004; Lee et al., 2004b; Harasaki et al., 2005; Tang et al., 2005; Traub, 2005; Richter et al., 2009; Foresti et al., 2010).

In the conventional view of vacuolar or lysosomal trafficking in various eukaryotic cells, the sorting of vacuolar/lysosomal proteins occurs at the TGN (Bonifacino and Rojas, 2006; Pfeffer, 2007; Hwang, 2008). Mannose 6-phosphate receptors and vacuolar protein sorting 10 (Vps10p) are involved in the sorting in animal and yeast cells, respectively (Gabel et al., 1982; Marcusson et al., 1994; Arighi et al., 2004; Bonifacino and Rojas, 2006). In plant cells, proteins known as vacuolar sorting receptors (VSRs) are involved in this process. In *Arabidopsis thaliana*, seven VSR isoforms have been identified (Ahmed et al., 1997; Shimada et al., 2003; Zouhar et al., 2010). They are type I membrane proteins and are highly conserved in different plant species (Kirsch et al., 1994, 1996; Ahmed et al., 1997; Paris and Neuhaus, 2002). These cargo sorting receptors travel together with cargo proteins from the TGN to the late endosome or the PVC. Although certain sorting receptors, such as receptor homology region transmembrane domain ring H2 motif protein, travel together with their cargo to the final destination, VSRs might travel from the late endosome or PVC to the TGN for next-round sorting of the lysosomal or vacuolar proteins (Sanderfoot et al., 1998; Li et al., 2002; Tse et al., 2004; Park et al., 2005). In yeast and mammals, the retromer is thought to be involved in the recycling of VPS10p and mannose 6-phosphate receptors, respectively, from the PVC/late endosomes to the TGN (Seaman et al., 1997, 1998; Arighi et al., 2004; Seaman, 2004). The retromer comprises five subunits, which form two subcomplexes (Seaman et al., 1998). VPS26, VPS35, and VPS29 form one of these subcomplexes, called the cargo-selective subcomplex, which binds to cargoes via VPS35 (Nothwehr et al., 2000). The other subcomplex comprises sorting nexin

[1] Address correspondence to ihhwang@postech.ac.kr.
The author responsible for the distribution of materials integral to the findings presented in this article in accordance with the policy described in the Instructions for Authors (www.plantcell.org) is: Inhwan Hwang (ihhwang@postech.ac.kr).
[W] Online version contains Web-only data.
www.plantcell.org/cgi/doi/10.1105/tpc.112.103481

(SNX) dimers (Vps5p/17p in yeast and SNX 1/2 in mammals and plants), which directly bind to phosphatidylinositol 3-phosphate and are involved in membrane remodeling (Collins, 2008; Cullen, 2008). In plants, several lines of evidence support the notion that the retromer complex also is involved in the retrieval of *Arabidopsis* VSRs. The VPS35/29/26 subcomplex is a stable trimer, and VPS35 coimmunoprecipitates with *Arabidopsis* VSRs (Oliviusson et al., 2006). In addition, all the subunits within this complex localize to the PVC (Oliviusson et al., 2006). Recently, however, a new working model of the retromer complex was proposed based on the different localization of sorting nexin and cargo-selective subcomplexes at the TGN and the PVC, respectively (Oliviusson et al., 2006; Niemes et al., 2010b). In this model, it was suggested that recycling of VSRs occurs from the TGN to the ER, VSR may exit the ER via COPII-independent manner, and transport of vacuolar cargoes from the TGN might be achieved by maturation of the TGN to the PVC (Niemes et al., 2010a, 2010b). However, this model brings new questions, such as how the vacuolar transport pathway is separated from the secretory pathway at the TGN in plant cells (De Marcos Lousa et al., 2012; Robinson et al., 2012).

Arabidopsis VPS29 is involved in the trafficking of seed storage proteins destined for the PSV in *Arabidopsis* seed cells, as well as in vegetative growth (Shimada et al., 2006). The phenotypes of *mag1-1* plants, which harbor a T-DNA insertion into the 3′-untranslated region of *Arabidopsis VPS29*, resulting in a *VPS29* knockdown mutation, indicate an important role for VPS29 in plant growth; however, it is not known how severe reduction of *VPS29* expression causes defects in vegetative growth at the molecular level. Based on defects observed in seed cells and the known function of VPS29 in animal and yeast cells (Seaman et al., 1997, 1998; Arighi et al., 2004), one possible explanation is that lower levels of VSP29 in *mag1-1* mutants cause a defect in protein trafficking, which in turn leads to defects in vegetative growth. However, whether *mag1-1* mutant plants have a defect in protein trafficking in vegetative tissues is rather difficult to test genetically at the whole plant level. Despite the possible caveats caused by the absence of the cell wall, and if properly used, the protoplast system offers a unique opportunity to dissect the physiological role(s) played by the molecular machinery involved in protein trafficking (Jin et al., 2001; Kim et al., 2001; Song et al., 2006; Lee et al., 2007; Denecke et al., 2012). Therefore, in this study, we used a protoplast system to dissect the effects of *mag1-1* on protein trafficking in vegetative cells. We present evidence that *Arabidopsis* VPS29 is involved in the recycling of VSR1 from the PVC to the TGN during the trafficking of soluble proteins to the LV. We also show that overexpression of VSR1:HA partially compensates for the lower levels of VPS29 in *mag1-1* mutant plants.

RESULTS

Trafficking of Soluble Proteins to the Vacuole Is Inhibited in *mag1-1* Mutant Plants

To test whether *mag1-1* mutant plants have a defect in protein trafficking, we first examined vacuolar trafficking in protoplasts from leaf tissues. Protoplasts from wild-type or *mag1-1* plants were transformed with *sporamin*:*green fluorescent protein* (*Spo*:*GFP*), a chimeric LV-targeted protein fusion of sporamin from sweet potato (*Ipomoea batatas*) and GFP (Jin et al., 2001; Kim et al., 2001). The majority of wild-type protoplasts expressing Spo:GFP showed a vacuolar localization pattern, with a small proportion exhibiting the network and spot pattern reported previously (Sohn et al., 2003; Tamura et al., 2005). However, *mag1-1* protoplasts showed a clearly different localization pattern; the majority of *mag1-1* protoplasts produced a punctate staining pattern with a minor portion showing the vacuolar pattern (Figure 1A). We quantified the localization pattern of Spo:GFP to assess the differences between wild-type and *mag1-1* mutant protoplasts. In the wild type, 71% of protoplasts expressing Spo:GFP showed the vacuolar pattern, whereas only 41% of *mag1-1* protoplasts showed this pattern (Figure 1B), indicating that the *mag1-1* mutation causes a defect in the trafficking of Spo:GFP to the LV. This localization pattern might be underestimated because GFP proteins in the LV are degraded in light conditions (Tamura et al., 2003). However, in spite of the possibility for underestimate of localization pattern or trafficking efficiency, there was a marked difference in protein localization between wild-type and *mag1-1* plants.

To obtain supporting evidence for this, we examined the trafficking of another vacuolar luminal protein, AALP:GFP, a chimeric protein consisting of *Arabidopsis* aleurain-like protein (AALP) and GFP (Sohn et al., 2003). Again, the majority (84%) of wild-type protoplasts expressing AALP:GFP showed GFP fluorescence signals in the vacuole (Figures 1A and 1B). By contrast, the majority (65%) of *mag1-1* protoplasts showed a punctate staining pattern, with only a minor proportion (35%) showing the vacuolar pattern (Figures 1A and 1B); this confirmed that the trafficking of AALP:GFP to the LV is defective in *mag1-1* mutant plants.

To confirm these results at the biochemical level, we next determined the trafficking efficiency of Spo:GFP and AALP:GFP to the vacuole in wild-type and *mag1-1* protoplasts. *Spo*:*GFP* or *AALP*:*GFP* was introduced into wild-type or *mag1-1* protoplasts, and proteins extracted from transformed protoplasts and from the incubation medium were analyzed by immunoblotting with an anti-GFP antibody. Spo:GFP generated two protein bands at 36 and 30 kD in protoplasts; these bands represent full-length Spo:GFP and its proteolytically cleaved form, respectively (Sohn et al., 2003). In the incubation medium, a 30.5-kD protein band was detected. The 30.5-kD secreted protein was also detected when a dominant-negative form of Rha1 was overexpressed; this 30.5-kD protein might be generated by proteolysis of Spo:GFP by proteases present in the medium (Matsuoka et al., 1995; Sohn et al., 2003). Similarly, AALP:GFP produced two bands at 70 and 30 kD, which correspond to the full-length and processed forms, respectively. Trafficking efficiency was determined according to the ratio of the amount of the processed form to the total amount of expressed protein. In addition, the degree of protein secretion into the incubation medium was determined. In wild-type protoplasts, the trafficking efficiency of both Spo:GFP and AALP:GFP increased with time, reaching 75 and 68%, respectively, at 36 h after transformation (HAT). By contrast, the trafficking efficiency of Spo:GFP and AALP:GFP in *mag1-1* protoplasts decreased to 45 and 41%, respectively, at 36 HAT. Moreover, Spo:GFP and

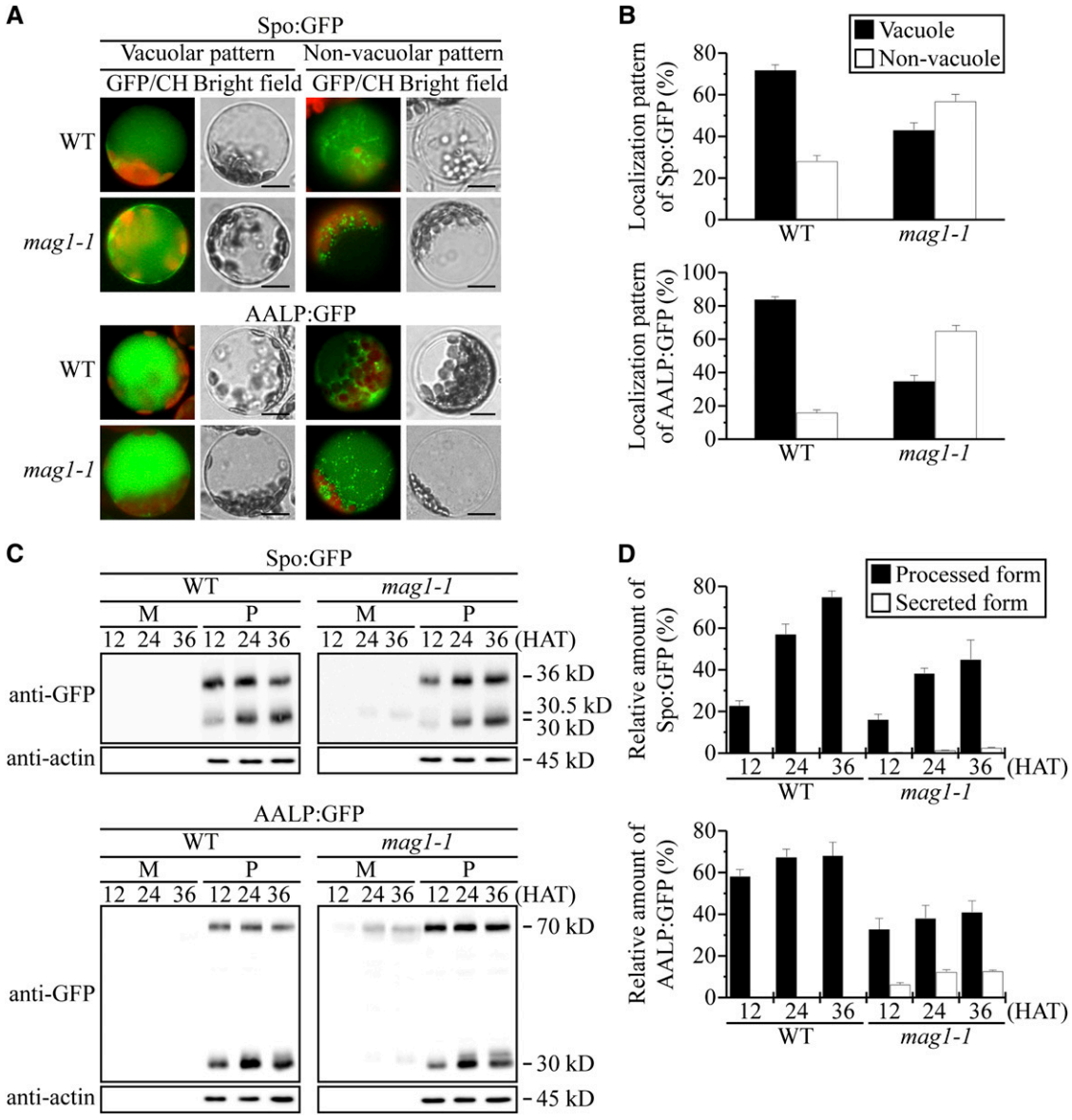

Figure 1. *mag1-1* Mutants Show a Defect in the Trafficking of Soluble Proteins to the LV in Vegetative Tissues.

(A) A defect in the trafficking of Spo:GFP and AALP:GFP in *mag1-1* protoplasts. Protoplasts from leaf tissues of wild-type (WT) or *mag1-1* mutant plants were transformed with *Spo*:*GFP* (10 μg) or *AALP*:*GFP* (10 μg), and the trafficking of these proteins to the vacuole was examined by in vivo imaging. Images of transformed protoplasts were acquired 24 HAT. CH, red autofluorescence of chlorophyll. Bar = 20 μm.

(B) Quantification of localization patterns. To assess trafficking efficiency, the localization of Spo:GFP or AALP:GFP in wild-type or *mag1-1* protoplasts was quantified. To quantify the localization pattern, the following criteria were applied: Protoplasts showing a vacuolar staining pattern with three or less than three punctate stains per protoplast (vacuolar pattern shown in **[A]**) were considered to have a vacuolar pattern, whereas protoplasts with more than four punctate stains per protoplast were considered to have a nonvacuolar pattern (nonvacuolar pattern shown in **[A]**), even if they showed a weak vacuolar staining pattern. In most cases, when protoplasts showed a punctate staining pattern, the number of punctate stains was >10 per protoplast. Three independent transformation experiments were performed for each construct, and more than 50 transformed protoplasts were counted each time. Error bars represent the SD (n = 3).

(C) and **(D)** Trafficking efficiency in *mag1-1* mutant plants. Protoplasts from wild-type or *mag1-1* plants were transformed with *AALP*:*GFP* (10 μg) or *Spo*:*GFP* (10 μg), and protein extracts were prepared at the indicated time points. Proteins from the incubation medium were included.

(C) Immunoblot analysis was performed with an anti-GFP antibody. Actin levels were detected with an antiactin antibody to use as a loading control as well as a control for the contamination of cytosolic proteins to the incubation medium. M, medium; P, protoplasts.

(D) Quantification of trafficking efficiency in *mag1-1* mutant plants. To quantify the trafficking efficiency of AALP:GFP and Spo:GFP, the signal intensity of full-length, processed, and secreted proteins on immunoblots was measured by a software-equipped LAS3000, and the intensity of the

AALP:GFP secreted into the medium was 3 and 12%, respectively, of the total expressed protein (Figures 1C and 1D), confirming that vacuolar trafficking of Spo:GFP and AALP:GFP is inhibited in *mag1-1* mutants. Actin (detected by an antiactin antibody) was used as a loading control.

The inhibitory effect of the *mag1-1* mutation on vacuolar trafficking was stronger with AALP:GFP than Spo:GFP and had a different temporal inhibition pattern. The inhibitory effect of the *mag1-1* mutation on the vacuolar trafficking of AALP:GFP was observed from early time points after transformation, such as 12 HAT. By contrast, the inhibitory effect of the *mag1-1* mutation on vacuolar trafficking of Spo:GFP was not observed at 12 HAT but was detectable 24 or 36 HAT. This difference in the degree of inhibition and the temporal inhibition pattern between AALP:GFP and Spo:GFP in the *mag1-1* protoplasts may be caused by the difference in their rate of exit from the ER. In wild-type protoplasts, AALP:GFP was targeted to the vacuole faster than Spo:GFP (Figure 1D). Indeed, trafficking efficiency of Spo:GFP was low at 12 HAT and reached to over 50% at 24 or 36 HAT. Consistent with this idea, strong GFP signals were observed in the ER during early time points, raising the possibility that ER exit of Spo:GFP is a rate-limiting step in vacuolar trafficking. Thus, one possible explanation is that the low levels of VSRs at the TGN in *mag1-1* protoplasts may be able to properly sort a small amount of Spo:GFP reaching the TGN at early time points after transformation but may have difficulty sorting a large amount of Spo:GFP reaching the TGN at 24 or 36 HAT for vacuolar trafficking.

mag1-1 Mutants Do Not Exhibit Defective Trafficking of Membrane Proteins to the LV and Plasma Membrane or Secretion into Apoplasts

To gain further insight into the physiological role of VPS29 during trafficking of proteins in the cells of vegetative tissues, we examined the trafficking of membrane proteins to the vacuole. βFruct4:GFP, a fusion between *Arabidopsis* βFructosidase4 (βFruct4) and GFP, is targeted as a membrane protein to the vacuole from the ER via the Golgi apparatus and the PVC. However, when the fusion protein arrived at the LV, the GFP moiety (and possibly the mature domain of βFruct4) was proteolytically processed and released from the tonoplast into the lumen of the vacuole, thereby showing a luminal localization pattern (Jung et al., 2011). The N-terminal fragment containing 84 amino acids of βFruct4 (FN) is sufficient to target a GFP fusion protein (FN:GFP) to the LV in a manner identical to the full-length fusion protein βFruct4:GFP. Protoplasts from wild-type and *mag1-1* plants were transformed with *FN:GFP* and its localization was examined. Approximately 66% of wild-type protoplasts expressing FN:GFP showed the vacuolar pattern, together with a minor proportion (34%) that showed the network and punctate staining pattern. Similarly, FN:GFP showed a vacuolar pattern in 64% of *mag1-1* protoplasts (Figures 2A and 2B), indicating that the *mag1-1* mutant does not have a defect in trafficking FN:GFP to the vacuole. To support this at the biochemical level, the trafficking efficiency of FN:GFP was examined by immunoblotting using proteins extracted from wild-type or *mag1-1* protoplasts transformed with *FN:GFP* with an anti-GFP antibody. Binding protein (BiP) levels were monitored as a loading control using an anti-BiP antibody (Lee et al., 2004a; Kim et al., 2005). FN:GFP generated two protein bands at 40 and 30 kD, which corresponded to the full-length and vacuolar-processed forms of FN:GFP, as observed previously (Jung et al., 2011). In both wild-type and *mag1-1* protoplasts, the 30-kD processed protein predominated over the full-length protein, and the ratios of the full-length and processed forms did not differ (Figure 2C), indicating that the trafficking of membrane protein βFruct4 to the vacuole was not affected in the *mag1-1* mutant. These results suggest that VPS29 is involved only in the trafficking of luminal proteins to the LV. To further confirm that the targeting of vacuolar membrane proteins is not affected in *mag1-1*, we examined trafficking of TPK1, an *Arabidopsis* tandem-pore potassium channel family protein, which is targeted to the tonoplast via the Golgi apparatus (Dunkel et al., 2008). A TPK1-YFP (for yellow fluorescent protein) fusion was expressed in wild-type or *mag1-1* protoplasts and its localization was examined. TPK1:YFP localized to the tonoplast in both the wild type and *mag1-1* (see Supplemental Figure 1 online), confirming that VPS29 is not involved in the trafficking of vacuolar membrane proteins.

To further test the specificity of VPS29 in protein trafficking, we examined the trafficking of invertase:GFP and H^+-ATPase:GFP as representative secretory and plasma membrane proteins, respectively (Kim et al., 2005). Invertase:GFP is a fusion between secretory apoplastic invertase and GFP, and H^+-ATPase:GFP is a fusion between plasma membrane H^+-ATPase and GFP (Kim et al., 2005). Proteins extracted from wild-type and *mag1-1* protoplasts transformed with *invertase:GFP* and from the incubation medium were subjected to immunoblot analysis with an anti-GFP antibody. The amounts of invertase:GFP secreted into the incubation medium by wild-type and *mag1-1* protoplasts were almost the same, indicating that VPS29 is not involved in protein secretion (Figure 2D). Next, *H^+-ATPase:GFP* was transformed into wild-type and *mag1-1* protoplasts and its localization examined by fluorescence microscopy. H^+-ATPase:GFP localized to the plasma membrane in wild-type and *mag1-1* protoplasts (Figure 2E), indicating that the trafficking of proteins to the plasma membrane was not inhibited in *mag1-1* protoplasts.

mag1-1 Severely Reduced the Capacity of the Trafficking Pathways for Vacuolar Luminal Proteins

The *mag1-1* plants showed much milder defects in plant growth than null mutant *mag1-2* mutants, which have a T-DNA insertion in the third exon of *VPS29* (Shimada et al., 2006), raising the

Figure 1. (continued).

processed or secreted forms was expressed as a value relative to that of the total amount of expressed protein. Three independent transformations were performed. Error bars represent the SD ($n = 3$).

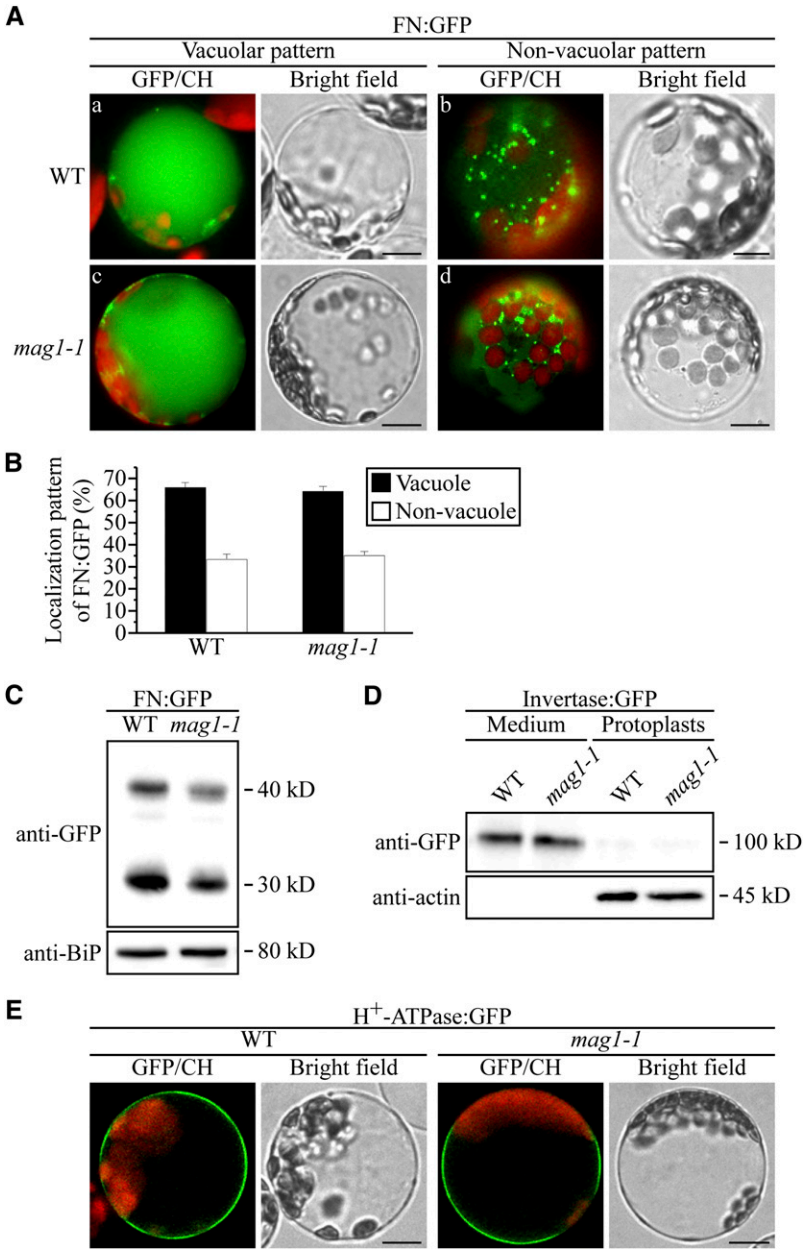

Figure 2. *mag1-1* Mutant Plants Do Not Affect the Trafficking of Membrane Proteins to the Vacuole and Plasma Membrane or into the Secretory Pathway.

(A) to **(C)** The *mag1-1* mutation has no effect on the trafficking of FN:GFP. **(A)** Protoplasts from leaf tissues from wild-type (WT) or *mag1-1* mutant plants were transformed with *FN*:*GFP*, and the localization of FN:GFP was determined by fluorescence microscopy at 24 HAT. CH, red autofluorescence of chlorophyll. Bars = 20 μm.

(B) The localization pattern of FN:GFP was quantified by counting protoplasts in panels **(a)**/**(c)** or panels **(b)**/**(d)** in **(A)**. Protoplasts showing a vacuolar pattern with three or less than three punctate stains per protoplast were considered to have a vacuolar pattern (as shown in **[a]** and **[c]**), and protoplasts with more than three punctate stains per protoplast and/or network pattern were considered to have a nonvacuolar pattern (as shown in **[b]** and **[d]**). Three independent transformation experiments were performed and 50 different protoplasts were analyzed for their localization pattern each time. Error bars represent the SD (n = 3).

(C) Trafficking of FN:GFP was also examined by immunoblot analysis with an anti-GFP antibody. BiP was used as a loading control.

(D) The *mag1-1* mutation has no effect on the secretion of invertase:GFP. Protoplasts from leaf tissues of wild-type or *mag1-1* mutant plants were transformed with *invertase*:*GFP*, and trafficking efficiency was determined at 24 HAT by immunoblot analysis with an anti-GFP antibody. Proteins from the incubation medium were included. Actin was used as a loading control.

possibility that lower levels of VPS29 may still be able to manage vacuolar trafficking, albeit at reduced capacity. To test this idea, we took advantage of one feature of the protoplast system, wherein the amount of cargo protein loaded into the trafficking pathway in protoplasts can be varied substantially by introducing different amounts of plasmid DNA encoding specific proteins. Initially, we examined how much protein can be transported to the vacuole in protoplasts from wild-type plants. Protoplasts from the leaf tissues of wild-type plants were transformed with varying amounts of *AALP*:*GFP* plasmid DNA, and proteins extracted from the protoplasts and from the incubation medium were analyzed by immunoblotting with an anti-GFP antibody. The incubation medium was analyzed because excess protein loaded into the vacuolar trafficking pathway is secreted into the incubation medium via a default pathway (Frigerio et al., 1998; Sohn et al., 2003). The amount of total and processed AALP:GFP increased by 2.6- and 1.7-fold, respectively, as the amount of *AALP:GFP* increased from 10 to 30 μg (Figures 3A and 3B), and a negligible amount of AALP:GFP was detected in the incubation medium only at 30 μg of AALP:GFP. These results strongly suggest that the wild-type protoplasts have the capacity to transport proteins to the LV in amounts almost equivalent to that induced by the expression of 30 μg of *AALP*:*GFP* plasmid DNA. Next, *mag1-1* protoplasts were transformed with 10 to 30 μg of *AALP*:*GFP* plasmid DNA, and proteins extracted from the protoplasts and from the incubation medium were analyzed by immunoblotting with an anti-GFP antibody. The amounts of AALP:GFP expressed by *mag1-1* protoplasts were comparable with those by wild-type protoplasts, indicating that *mag1-1* protoplasts do not show defective protein expression. The amount of the processed form of *AALP*:*GFP* detected in *mag1-1* protoplasts also increased with increasing amounts of *AALP*:*GFP* DNA but not to levels comparable with those in wild-type protoplasts. Interestingly, the smaller increase in the amount of the processed form resulted in the accumulation of full-length AALP:GFP and in the secretion of AALP:GFP into the incubation medium, indicating that the capacity of the trafficking pathway to transport soluble proteins to the vacuole is greatly reduced in *mag1-1* mutant protoplasts.

We next tested this finding with Spo:GFP. Again, the expression levels of Spo:GFP were almost comparable in both wild-type and *mag1-1* protoplasts. Next, we compared the trafficking efficiency in both types of protoplast. In wild-type and *mag1-1* protoplasts, the increase in Spo:GFP expression resulted in a concomitant increase in the levels of its processed form. However, there was a difference in the extent of the increase (Figures 3A and 3B). In wild-type protoplasts, the amount of the processed form increased to the same extent as that of Spo:GFP. By contrast, the extent of the increase in the amount of the processed form in *mag1-1* protoplasts was roughly half that in wild-type protoplasts, and the remaining proteins accumulated as full-length proteins that were not secreted, confirming that *mag1-1* mutant plants have a reduced capacity to traffic soluble proteins to the vacuole.

Vacuolar Soluble Cargoes Are Trapped at the TGN on the Way to Their Final Destinations

In *mag1-1* protoplasts, although a significant amount of AALP:GFP was secreted into the medium, both Spo:GFP and AALP:GFP mainly showed punctate staining patterns, indicating that they were temporarily trapped in intermediate compartments en route to the LV. The intermediate compartments in the vacuolar trafficking pathway from the ER are the Golgi apparatus, the TGN, and the PVC. Therefore, to identify the intermediate compartments in which these proteins were trapped, we compared the localization of Spo:GFP or AALP:GFP with that of organelle markers. We used KAM1(ΔC):mRFP, a chimeric fusion between Katamari1 (KAM1) harboring a C-terminal deletion and monomeric red fluorescent protein (mRFP); this fusion localizes to the *cis*-Golgi apparatus (Tamura et al., 2005; Lee et al., 2011), SYP61, a t-SNARE localized to the TGN (Sanderfoot et al., 2001; Uemura et al., 2004), and HA-tagged PEP12p, a t-SNARE localized to the PVC (Sanderfoot et al., 1998; Kim et al., 2010), as organelle marker proteins. *KAM1(ΔC):mRFP* or *PEP12p*:*HA* were cotransformed into *mag1-1* protoplasts together with *Spo*:*GFP* or *AALP*:*GFP* and their localization was examined directly or by immunostaining with an anti-HA antibody or an anti-SYP61 antibody. Previously, overexpression of PEP12p/SYP21 has been shown to inhibit vacuolar trafficking and cause accumulation of vacuolar cargoes to the PVC (Foresti et al., 2006). Therefore, before we performed colocalization experiments, we determined the amount of plasmid DNA encoding PEP12p:HA or GFP:SYP21 that did not compromise the trafficking of AALP:GFP and Spo:GFP. The vacuolar trafficking of AALP:GFP and Spo:GFP was not affected with 5 or 2 μg of *PEP12p*:*HA* and of *GFP*:*SYP21*, respectively (see Supplemental Figure 2 online). Using these conditions, we performed colocalization experiments. Of these three organelle marker proteins, the major proportion of Spo:GFP (60%) and AALP:GFP (58%) colocalized with SYP61, and a lower proportion with PEP12p:HA (Figures 4B to 4D). In addition, a minor proportion of Spo:GFP (5%) and AALP:GFP (6%) colocalized with KAM1(ΔC):mRFP (Figures 4A and 4D). However, a couple of punctate signals of Spo:GFP did not colocalize with any of the known organellar markers, indicating that a very minor proportion may also be targeted to an unidentified location. Together, these results indicate that AALP:GFP and Spo:GFP accumulate primarily in the TGN in *mag1-1* mutant protoplasts, with a minor proportion in the PVC and the Golgi apparatus on the way to their final destinations.

Recently, Foresti et al. (2010) identified the late prevacuolar compartment (LPVC) in tobacco (*Nicotiana tabacum*) leaf cells using a recycling defective VSR2, VSR2(L615A). In addition,

Figure 2. (continued).

(E) The *mag1-1* mutation has no effect on the targeting of H^+-ATPase:GFP to the plasma membrane. Protoplasts from leaf tissues of wild-type or *mag1-1* mutant plants were transformed with *H^+-ATPase*:*GFP*, and its localization was determined by fluorescence microscopy at 24 HAT. CH, red autofluorescence of chlorophyll. Bars = 20 μm.

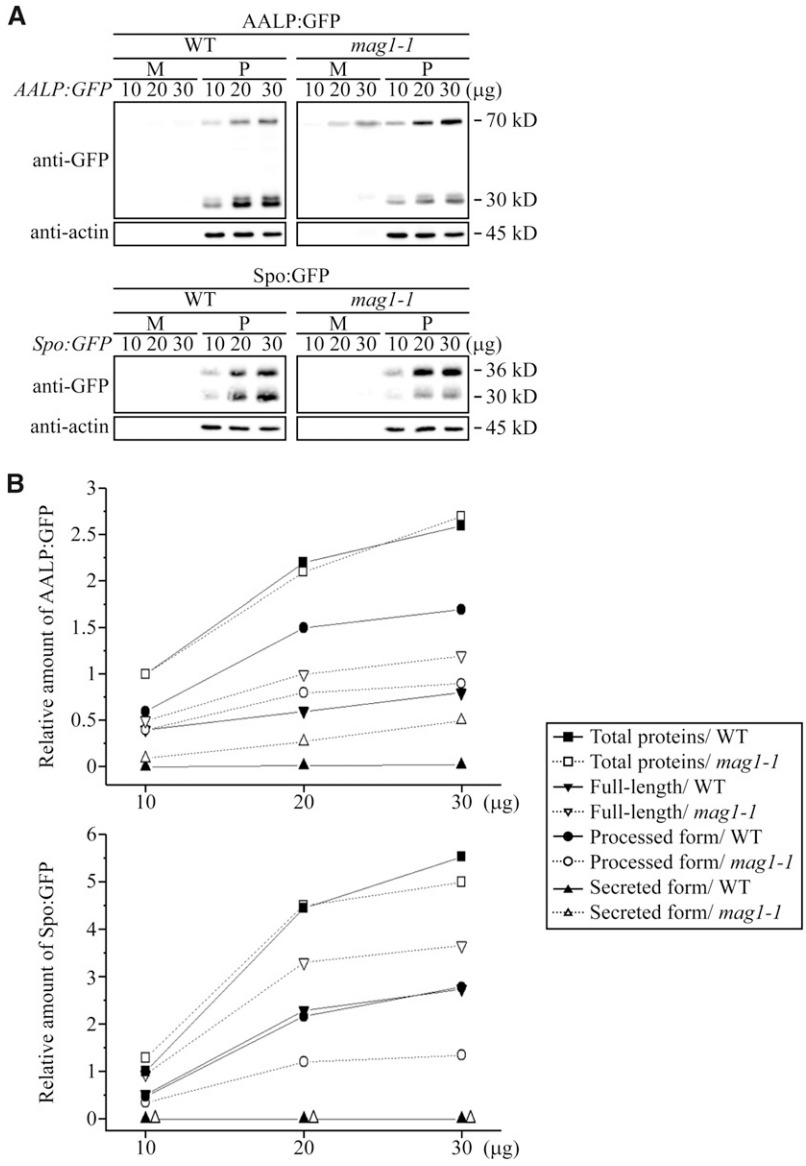

Figure 3. The Capacity of the Vacuolar Trafficking Pathway for Soluble Proteins Is Significantly Reduced in *mag1-1* Mutant Plants.

(A) Effect of AALP:GFP and Spo:GFP levels on vacuolar trafficking in *mag1-1* mutant protoplasts. Protoplasts from leaf tissues of wild-type (WT) and *mag1-1* plants were transformed with the indicated amounts of *AALP*:*GFP* or *Spo*:*GFP* plasmid DNA (10 to 30 μg), and the trafficking efficiency was determined by immunoblotting with an anti-GFP antibody at 24 HAT. Proteins from the incubation medium were included. Actin was used as a loading control as well as a control for contamination of cytosolic proteins to the incubation medium. M, medium; P, protoplasts.

(B) Quantification of trafficking capacity. The signal intensities of the protein bands in the immunoblot in **(A)** were measured as described in Figure 1D and expressed as values relative to the amount of total protein expressed in wild-type protoplasts transformed with 10 μg of *AALP*:*GFP* or *Spo*:*GFP*.

a vacuolar cargo Aleu-RFP colocalizes with GFP-VSR2(L615A) to the LPVC on the way to the vacuole. Accordingly, we examined whether vacuolar cargoes were trapped in the LPVC in *mag1-1* mutants. Initially, we examined the expression of myc-tagged *Arabidopsis* VSR1(L609A), VSR1(L609A):myc, in wild-type protoplasts by immunoblotting using anti-myc antibody (see Supplemental Figure 3A online). To determine the localization of VSR1(L609A) in wild-type or *mag1-1* protoplasts, *VSR1(L609A)*:*myc* was introduced into wild-type or *mag1-1* protoplasts together with *VSR1*:*HA* and their localization was examined by immunohistochemistry using anti-HA and anti-myc antibodies. VSR1(L609A):myc colocalized with wild-type VSR1:HA in both the wild type and *mag1-1* (see Supplemental Figure 3B online), indicating that in contrast with the previous result in tobacco leaf cells, *Arabidopsis* VSR1(L609A) localizes to the PVC. The difference in the localization of VSR1(L609A) in this and previous studies may be due to the difference in the plant species or experimental conditions, including the different classes of VSRs

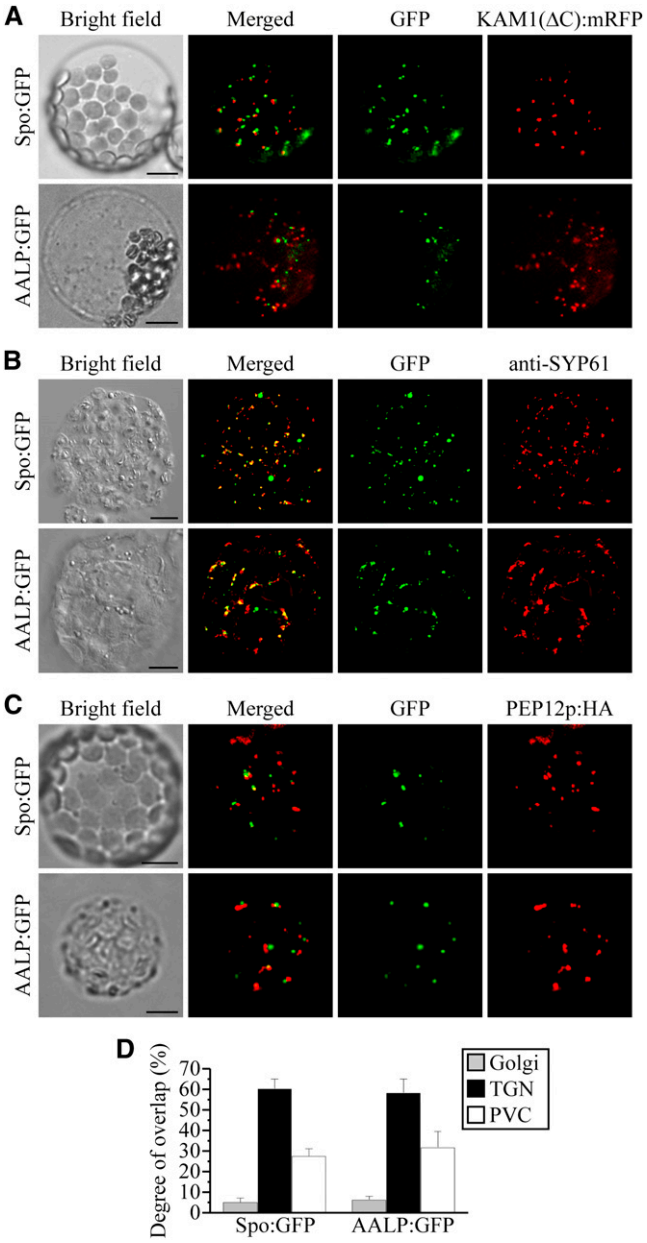

Figure 4. The *mag1-1* Mutants Show a Defect in Trafficking of Vacuolar Luminal Proteins from the TGN to the PVC.

(A) to **(C)** Colocalization of AALP:GFP and Spo:GFP with various organelle markers. *AALP:GFP* or *Spo:GFP* was cotransformed into *mag1-1* protoplasts together with *KAM1(ΔC):mRFP* **(A)** or *PEP12p:HA* (5 μg) **(C)**, and their localization was examined at 24 HAT directly by monitoring the fluorescence signals or by immunohistochemistry using an anti-HA or anti-SYP61 antibodies. As a TGN marker, SYP61 was detected by immunohistochemistry using anti-SYP61 antibody **(B)**.

(D) Quantification of colocalization. The degree of overlap between Spo:GFP or AALP:GFP and KAM1(ΔC):mRFP, SYP61, or PEP12p:HA was quantified in more than 50 protoplasts randomly selected from a population of protoplasts transformed with each of the fusions. Three independent transformation experiments were performed. Error bar represents the SD (n = 3).

used in these studies; in this study, we used *Arabidopsis* VSR1 (VSR1;1), which belongs to class I of VSRs, but the previous study used VSR2 (VSR2;1), which belongs to class 2 (De Marcos Lousa et al., 2012). With this finding, we next examined whether or not Spo:GFP or AALP:GFP colocalizes with VSR1(L609A):myc in *mag1-1* protoplasts. Only a minor proportion of Spo:GFP and AALP:GFP colocalized with VSR1(L609A):myc, confirming that vacuolar cargoes are trapped in the PVC, but not the LPVC on the way to their final destination in *mag1-1* mutants (see Supplemental Figure 3C online).

VSR1 Does Not Efficiently Recycle from the PVC to the TGN, but Relocates from the PVC to the Vacuole at Higher Rates in *mag1-1* Plants

To gain insight into the mechanism by which VSP29 acts in the vacuolar trafficking of soluble proteins, we examined the behavior of VSRs. VSRs play a crucial role in sorting soluble proteins at the TGN and recycle from the PVC to the TGN (Li et al., 2002; Tse et al., 2004; Kim et al., 2010), although a recent study proposed that VSRs recycle from the TGN to the ER, where they are involved in sorting vacuolar proteins (Niemes et al., 2010a). *Arabidopsis* VPS29 is a component of the retromer complex (Oliviusson et al., 2006; Shimada et al., 2006; Jaillais et al., 2007), which is thought to be responsible for recycling VSRs (Oliviusson et al., 2006). Initially, the localization of VSR1 was examined in protoplasts from *mag1-1* plants. Seven VSRs localize primarily to the PVC (Tse et al., 2004). To determine the localization of a specific VSR isoform, we used VSR1 tagged with HA (VSR1:HA) (Kim et al., 2010). *VSR1:HA* was cotransformed into protoplasts from wild-type or *mag1-1* mutant plants along with *GFP:SYP61* or *GFP:SYP21*, and the localization of these proteins was examined directly or by immunohistochemistry using anti-HA antibody. GFP:SYP61 and GFP:SYP21 were used as markers for the TGN and PVC, respectively (Uemura et al., 2004). GFP:SYP61 localized SYP61-positive compartments (see Supplemental Figure 4 online). In both wild-type and *mag1-1* protoplasts, the majority (>80%) of VSR1:HA closely colocalized with GFP:SYP21 and a small proportion (<20%) of VSR1:HA overlapped with GFP:SYP61 (Figures 5A and 5C), indicating that VSR1 primarily localizes to the PVC in both wild-type and *mag1-1* protoplasts as reported previously (Li et al., 2002; Tse et al., 2004; Kim et al., 2005, 2010). This result implied that, if VSRs recycle proteins for vacuolar trafficking, they would recycle from the PVC to the TGN. Accordingly, we tested whether VSR1:HA recycles from the PVC to the TGN by examining the localization of VSR1:HA in the presence of latrunculin B (LatB), a chemical compound that inhibits actin filament assembly. Previous studies demonstrated that LatB inhibits anterograde trafficking of VSR1 from the TGN to the PVC but allows retrograde trafficking from the PVC to the TGN, which in turn results in the accumulation of VSR1 at the TGN (Kim et al., 2005; Kim et al., 2010). *VSR1:HA* was cotransformed with *GFP:SYP61* or *GFP:SYP21*. Subsequently, at 22 HAT, they were treated with LatB and further incubated for 8 h. During the first 22 h incubation after transformation, the majority of VSR1:HA and cotransformed organellar markers would traffic normally to their final destinations, including the PVC. However, during the second 8 h incubation in the presence of LatB, the retrograde trafficking from the PVC

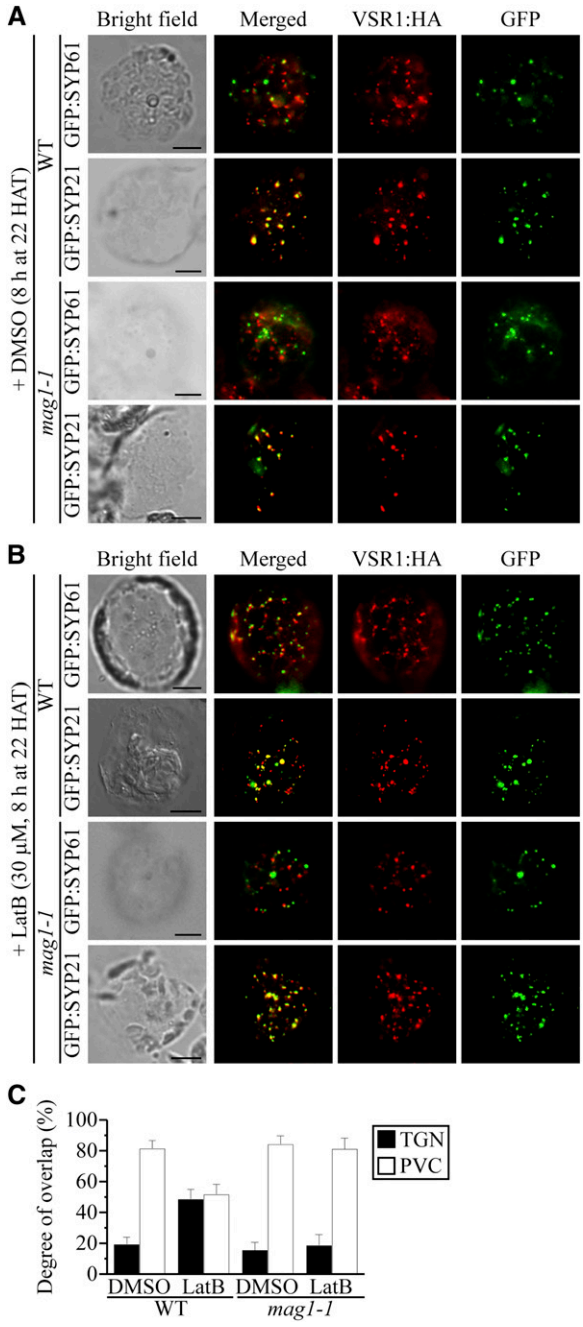

Figure 5. VSR1 Does Not Traffic Efficiently from the PVC to the TGN in *mag1-1* Plants.

(A) and **(B)** Localization of VSR1 in the presence of LatB. *VSR1:HA* was cotransformed into wild-type (WT) **(A)** or *mag1-1* **(B)** protoplasts together with *GFP:SYP61* or *GFP:SYP21*, and their localization was examined either by immunohistochemistry using an anti-HA antibody or directly by monitoring the green fluorescence signal. Transformed protoplasts were treated with LatB (30 μM) or DMSO at 22 HAT, followed by additional incubation for 8 h to inhibit anterograde trafficking of recycled VSR1:HA. DMSO, a vehicle used for LatB, was used for negative control.

(C) Quantification of VSR1 localization in the presence of LatB. To quantify the defect in the travel of VSR1 from the PVC to the TGN, the percentage of VSR1:HA-positive signals that overlapped with GFP:SYP61 or GFP:SYP21-positive speckles was determined in more than 50 protoplasts obtained from three independent transformation experiments. Bar indicates SD (n = 3).

to the TGN occurs, but the anterograde trafficking from the TGN to the PVC cannot occur (Kim et al., 2005). In the presence of LatB, the degree of overlap between VSR1:HA with GFP:SYP61 or GFP:SYP21in *mag1-1* protoplasts differed strikingly from that in wild-type protoplasts; in wild-type protoplasts, the overlap of VSR1:HA with GFP:SYP21 decreased to 51% (Figures 5B and 5C), similar to that in a previous report (Kim et al., 2005), whereas the degree of overlap was >80% in *mag1-1* protoplasts (Figures 5B and 5C), suggesting that VSR1:HA does not efficiently travel from the PVC to the TGN in *mag1-1* plants.

Next, we examined whether VSRs traffic from the PVC to the vacuole. In yeast *vps29*, *vps30*, and *vps35* mutants, the VSR, Vps10p, relocates from the late endosomes to the vacuole (Seaman et al., 1997). To test this, we used GFP:VSR1, a fusion protein generated by replacing the luminal domain of VSR1 with GFP, localized to the PVC in tobacco Bright Yellow-2 cells (Miao et al., 2006). Wild-type or *mag1-1* protoplasts were transformed with *GFP:VSR1* and the localization of the protein was examined over time. At 24 HAT, GFP:VSR1 showed a punctate staining pattern in ~50% of both wild-type and *mag1-1* protoplasts (Figures 6A and 6B). However, at 48 HAT, the percentage of protoplasts showing a punctate staining pattern was significantly lower in *mag1-1* protoplasts (15%) than in wild-type protoplasts (30%) (Figures 6A and 6B). To confirm the microscopy results at the biochemical level, wild-type or *mag1-1* protoplasts transformed with *GFP:VSR1* were harvested at 24 and 48 HAT, and protein extracts from the protoplasts were analyzed by immunoblotting using anti-GFP antibody. At 24 HAT, the amount of the GFP domain derived from GFP:VSR1 by proteolysis was similar in wild-type and *mag1-1* protoplasts. However, at 48 HAT, the amount of the GFP domain was significantly higher in *mag1-1* protoplasts than in wild-type protoplasts, confirming that GFP:VSR1 traffics from the PVC to the vacuole at a higher rate in *mag1-1* mutant protoplasts as observed with Vps10p in yeast retromer mutants (Seaman et al., 1997). One possible explanation is that the failure of GFP:VSR1 recycling from the PVC to the TGN results in enhanced trafficking of GFP:VSR1 from the PVC to the vacuole. Consistent with this, a mutant form of VSR1, which is defective in recycling, is efficiently transported to the vacuole (Foresti et al., 2010; Saint-Jean et al., 2010). These results strongly support the notion that VPS29 is involved in the recycling of VSRs from the PVC to the TGN.

Overexpression of VSR1 Rescues the Inhibitory Effect of the *mag1-1* Mutation on Vacuolar Trafficking in Protoplasts

To further test the idea that a failure to recycle VSRs from the PVC to the TGN is responsible for inhibiting the vacuolar trafficking of soluble proteins in *mag1-1* plants, we examined whether overexpression of VSR1 rescues the defect. The rationale for this idea was that high levels of newly synthesized VSR1 arriving in the TGN may be involved in sorting vacuolar proteins at the TGN, thereby supporting trafficking of vacuolar proteins from the TGN to the PVC. Indeed, a similar approach was used in a previous

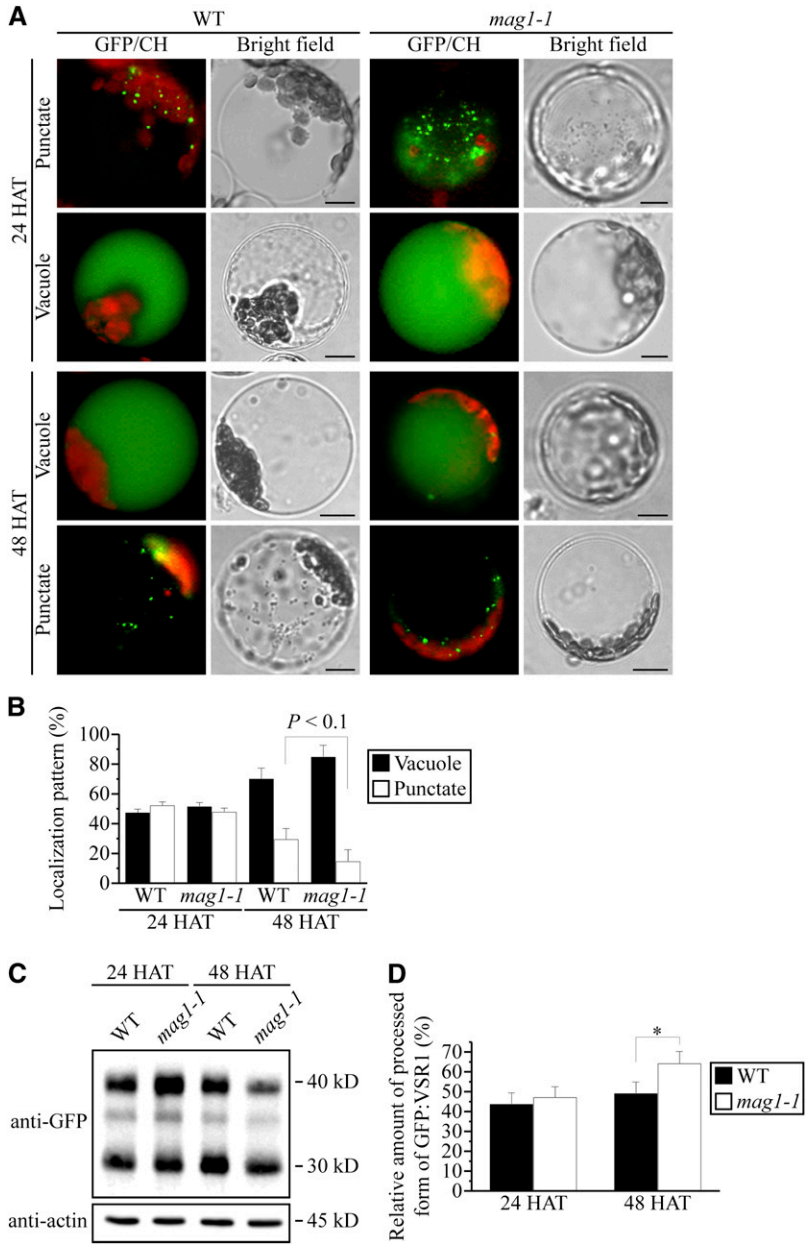

Figure 6. Trafficking of GFP:VSR1 from the PVC to the LV Occurs at Higher Rates in *mag1-1* Mutant Plants.

(A) Localization pattern of GFP:VSR1. Protoplasts from the leaf tissues of wild-type (WT) or *mag1-1* plants were transformed with *GFP*:*VSR1*, and its localization was determined at 24 or 48 HAT. CH, red autofluorescence of chlorophyll.

(B) Quantification of localization patterns. To examine the extent of the defect, the number of protoplasts showing the vacuolar and punctate staining patterns shown in **(A)** was counted. Protoplasts showing a vacuolar pattern with three or less than three punctate stains per protoplast were considered to have a vacuolar pattern, and protoplasts with more than three punctate stains per protoplast were considered to have a punctate staining pattern. However, the majority of protoplasts showing the punctate staining pattern contain more than five punctate stains per protoplasts. Error bars represent the SD (n = 3).

(C) Temporal expression pattern of GFP:VSR1. *GFP*:*VSR1* was transformed into wild-type or *mag1-1* protoplasts, and protein extracts from both protoplasts at indicated time points were analyzed by protein gel blotting using anti-GFP antibody. As a loading control, actin was detected with antiactin antibody.

(D) Quantification of proteolysis of GFP:VSR1. To quantify the proteolysis of GFP:VSR1 in the vacuole, the signal intensity of full-length and processed GFP bands on immunoblots was measured, and the intensity of the processed GFP band was expressed relative to that of the total amount of expressed protein. Three independent transformations were performed. Error bars represent the SD (n = 3). *P < 0.05.

study (daSilva et al., 2005). To test this idea, increasing amounts of *VSR1*:*HA* were cotransformed into protoplasts from wild-type or *mag1-1* plants along with a fixed amount of *AALP*:*GFP*, and the trafficking efficiency of AALP:GFP was determined by immunoblotting with an anti-GFP antibody. Proteins from the incubation medium were included in the analysis. Actin was detected as a control for nonspecific contamination of the incubation medium by cytosolic proteins and as a loading control. The expression of VSR1:HA was determined using an anti-HA antibody. In wild-type protoplasts, VSR1:HA did not have a noticeable effect on the trafficking of AALP:GFP to the LV (Figure 7A). By contrast, the trafficking efficiency of AALP:GFP in *mag1-1* protoplasts gradually increased, and the amount of secreted AALP:GFP gradually decreased as the amount of VSR1:HA increased (Figures 7A and 7B). This indicated that transiently expressed VSR1:HA compensates for the defect in the vacuolar trafficking of soluble proteins in *mag1-1* plants. These results support the idea that the recycling of VSR1, mediated by VPS29, is crucial for efficient trafficking of soluble proteins to the LV in vegetative cells.

Transcription of *VSRs* Is Induced but VSR Proteins Are Maintained at the Same Level in *mag1-1* Plants

The higher rate of trafficking of GFP:VSR1 to the vacuole in *mag1-1* plants compared with that in wild-type plants raised the possibility that VSR protein levels are lower in *mag1-1* plants than in wild-type plants, which in turn may contribute to the defect in trafficking of soluble vacuolar proteins from the TGN to the PVC. Indeed, in yeast cells, retromer mutants exhibit increased degradation of Vps10p in the vacuole (Seaman et al., 1997). To test this possibility, protein extracts from wild-type and *mag1-1* plants were analyzed by immunoblotting with an anti-VSR antibody. Unexpectedly, VSR levels were identical in wild-type and *mag1-1* mutant plants (Figure 8A). There may be two explanations for this. One is that, in contrast with GFP:VSR1, endogenous VSR proteins are not transported to the vacuole at higher rates in *mag1-1* plants than in wild-type plants. Another possibility is that *VSR* transcript levels are increased in *mag1-1* plants compared with those in wild-type plants. Indeed, a previous study demonstrated that the expression of a mutant form of *Arabidopsis* VSR1, VSR1 C2A:HA, in transgenic plants affects the transcription of endogenous *VSR1* (Kim et al., 2010). To distinguish between these possibilities, we determined the transcript levels of four *VSR* isoforms, *VSR1*, *VSR4*, *VSR5*, and *VSR6*, by quantitative RT-PCR. Interestingly, all four *VSR* isoforms were expressed at higher levels, the highest being *VSR1* (Figure 8B). These results strongly suggest that endogenous VSRs are also subject to a higher rate of trafficking from the PVC to the LV in *mag1-1* plants and that the resulting decrease in VSR levels is compensated for by increased expression of these genes.

DISCUSSION

VPS29 Plays an Important Role in Trafficking of Lytic Vacuolar Soluble Proteins

This study exploited a protoplast system to identify the possible role played by *Arabidopsis* VPS29 in protein trafficking in vegetative tissues. The protoplast system allows easy manipulation of the expression levels of cargo proteins using differing amounts of plasmid DNA and easy monitoring of protein trafficking to various organelles, including the LV. Despite the possibility for heavier trafficking of cell wall proteins and other cell wall components used to regenerate the cell walls in protoplasts, they still showed a significant capacity to transport proteins to the vacuole. Furthermore, the reduction in the capacity of vacuolar trafficking, which resulted from the lower levels of VPS29 in *mag1-1* mutant plants, was readily demonstrated in protoplasts. Of course, it should be noted that the difference in the trafficking capacity observed between wild-type and mutant protoplasts may reflect relative, but not absolute, differences.

Genetic approaches have been used to show that *Arabidopsis* VSP29, a component of the retromer complex, is involved in the trafficking of seed storage proteins to the PSV in seed cells and plays a crucial role in vegetative growth (Shimada et al., 2006). Here, we provide evidence that VPS29 also plays a crucial role in the vacuolar trafficking of soluble proteins in vegetative tissues, similar to its role in protein trafficking to the PSV in seed cells. The vacuolar luminal proteins, AALP:GFP and Spo:GFP, mainly accumulated in the TGN in *mag1-1* protoplasts from leaf tissues but were also secreted into the incubation medium. This is reminiscent of the defects in trafficking of proteins to the PSV observed in seed cells from *mag1-1* plants: Unprocessed forms of 12S globulin and 2S albumin accumulate at higher levels and are secreted into the apoplast. Thus, one possible explanation for these defects in vacuolar trafficking is that vegetative cells in *mag1-1* mutants have a defect in the recycling of VSRs, similar to the defect proposed for seed cells.

Interestingly, the vacuolar soluble cargoes AALP:GFP and Spo:GFP accumulated in the TGN to a certain degree in *mag1-1* mutant plants (Figure 4), in addition to being secreted into the medium. The accumulation of cargoes in the TGN is rather intriguing because the VSR deficiency at the TGN should cause secretion of vacuolar proteins into the medium but not their accumulation to the TGN. Indeed, a significant proportion of vacuolar cargo was secreted into the medium in *mag1-1* protoplasts. One possible explanation for this discrepancy is that the secretory pathway was also affected by the *mag1-1* mutation. However, trafficking of secretory protein invertase:GFP and plasma membrane protein H^+-ATPase:GFP was not inhibited in *mag1-1* (Figures 2D and 2E), thus ruling out this possibility. Moreover, previous studies also showed that blocking of vacuolar trafficking at the TGN did not affect trafficking of invertase:GFP or H^+-ATPase:GFP at the post-ER compartments, including the TGN (Kim et al., 2005). Another more plausible possibility is that the *mag1-1* mutation affects recycling of not only VSRs, but also other regulatory molecules, such as v-SNARE, and tethering factors that are involved in anterograde trafficking from the TGN to the PVC. Thus, in the absence of these accessory proteins, vacuolar cargoes accumulate in the TGN. The third possibility is that VSRs below a certain threshold level at the TGN cannot efficiently form homomeric complexes, which are necessary for efficient packaging of cargoes into the anterograde vesicles. A previous study demonstrated that homomeric interaction of VSRs is important for efficient trafficking of vacuolar proteins at the TGN (Kim et al., 2010). It is possible that loading of VSRs together with bound

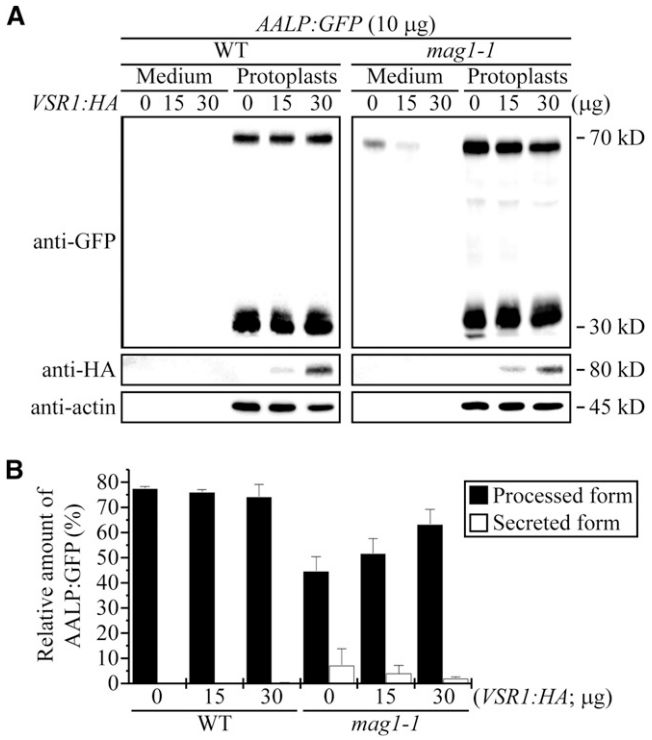

Figure 7. Transient Overexpression of VSR1 Complements the Defect of Vacuolar Trafficking in *mag1-1* Mutant Plants.

(A) Effect of overexpression of VSR1 on vacuolar trafficking of AALP:GFP in *mag1-1* plants. Varying amounts of *VSR1:HA* were cotransformed into protoplasts from the leaf tissues of wild-type (WT) or *mag1-1* mutant plants, together with a fixed amount (10 μg) of *AALP:GFP*, and the trafficking efficiency of AALP:GFP was determined at 24 HAT by immunoblotting using an anti-GFP antibody. Proteins from the incubation medium were included in the analysis. The expression level of VSR1:HA was determined by immunoblotting with an anti-HA antibody. Actin detected with an antiactin antibody was used as loading control as well as a control for the cytosolic protein contamination in the incubation medium.

(B) Quantification of trafficking efficiency. The trafficking efficiency was determined as described in Figure 1D. Error bars represent the SD (n = 3).

cargoes into budding vesicles occurs more efficiently as homomeric complexes compared with the monomeric form. In *mag1-1* plants, the amount of VSRs localized to the TGN may be below a threshold level so that the homomeric complex formation of VSRs may not occur rapidly. Thus, cargoes bound to monomeric VSRs may accumulate to the TGN transiently before they are packaged into the anterograde vesicle.

Newly Synthesized VSRs Partially Rescue the Vacuolar Trafficking of Soluble Protein in *mag1-1* Protoplasts

Results showing that in *mag1-1* mutant protoplasts, VSR1 did not efficiently recycle from the PVC to the TGN strongly suggest that a failure to recycle VSR1 is responsible for the defect in the vacuolar trafficking of soluble proteins. This hypothesis was tested using VSR1 overexpression in *mag1-1* mutant protoplasts. The underlying rationale for this approach was that, as long as VSR1 is provided to the TGN at high levels, either by retrograde trafficking from the PVC to the TGN or from the ER via de novo synthesis, the defect in the vacuolar trafficking at the TGN in *mag1-1* mutant protoplasts should be rescued. Indeed, overexpression of VSR1 rescued the defect in vacuolar trafficking of AALP:GFP in *mag1-1* protoplasts, supporting this hypothesis. Additional support for this hypothesis comes from the finding that the expression of *VSRs* was enhanced in *mag1-1* mutant plants. It is possible that the higher expression of *VSRs* resulted in increased amounts of nascent protein arriving at the TGN, which in turn compensated for the reduced level of VSRs coming from the PVC in *mag1-1* mutant plants, as we demonstrated by overexpressing VSR1 in protoplasts. A similar observation was made

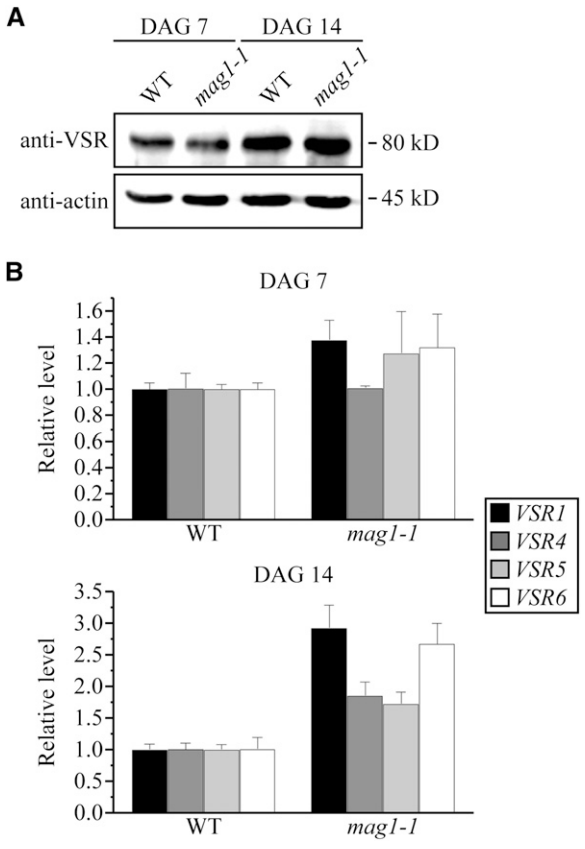

Figure 8. Expression of the Genes for Multiple At-*VSR* Isoforms Is Induced in *mag1-1* Mutant Plants.

(A) Immunoblot analysis of VSR protein levels. Protein extracts from 7- or 14-d-old wild-type (WT) or *mag1-1* plants were analyzed by immunoblotting using anti-VSR antibody. Actin levels were detected with antiactin antibody to use as a loading control as well as a control for the contamination of cytosolic proteins to the incubation medium. DAG, days after germination.

(B) Quantitative RT-PCR analysis of *VSR* transcript levels. Total RNA from 7- or 14-d-old plants was used for quantitative RT-PCR analysis using gene-specific primers. *Act2* and *Act8* were included as internal controls for quantitative RT-PCR. Error bars represent the SD (n = 3).

previously in transgenic plants expressing an *Arabidopsis* VSR1 mutant, VSR1:C2A, which harbors an Ala substitution in the C-terminal cytosolic tail, in a motif that is involved in the homomeric interaction between VSR1s. In transgenic plants harboring this mutant, the level of endogenous *VSR1* transcripts increased (Kim et al., 2010). In fact, this mechanism may compensate for the lower levels of VSR1 recycling in *mag1-1* plants. However, it is still not understood how the expression of *VSRs* is regulated in *mag1-1* mutant plants or in transgenic plants harboring the mutant form of *VSR1*. One possibility is that the cell has a mechanism for monitoring the VSR levels at the TGN. Recently, Chehab et al. (2007) reported that calcium-dependent protein kinase 1 (CPK1) interacts and colocalizes with CPK1 adaptor protein 2 (CAP2) at the VTI11-localized TGN in common ice plants (*Mesembryanthemum crystallinum*). Intriguingly, CAP2 shows a high degree of sequence similarity to the cytoplasmic domain of SNAREs but does not contain the transmembrane domain of SNAREs. CPKs, a gene family with 34 members in *Arabidopsis*, play a role in calcium sensing and are implicated in various biological processes, such as biotic and abiotic stress responses, transcriptional regulation, and pollen tube growth (DeFalco et al., 2009). Thus, one possible scenario is that these proteins may belong to a signaling circuit to induce expression of *VSRs* when the amount of VSRs does not match the levels of the cargoes. However, the exact mechanism remains to be studied in the future.

VSR1 Recycles from the PVC to the TGN in *Arabidopsis* Mesophyll Cells

Trafficking of proteins to the vacuole requires sorting of vacuolar proteins along the anterograde trafficking pathway, which is initiated at the ER. It is thought that sorting of vacuolar proteins occurs in the TGN. This idea is analogous with the trafficking of proteins to the lysosomes and vacuoles in animal and yeast cells, respectively (Bonifacino and Rojas, 2006; Pfeffer, 2007). Our results, showing that VSR1 fails to recycle to the TGN from the PVC in *mag1-1* mutant plants and that vacuolar proteins accumulate primarily in the TGN, strongly support the idea that vacuolar sorting occurs in the TGN. In addition, these results are consistent with previous studies on the localization of VSRs and sorting nexins. The majority of VSR1 localizes to the PVC with a minor proportion to the TGN (Li et al., 2002; Tse et al., 2004; Kim et al., 2005, 2010), and sorting nexins also localize to the PVC (Jaillais et al., 2006, Pourcher et al., 2010). However, recently, an alternative model for vacuolar cargo sorting by VSRs was proposed by Niemes et al. (2010a). In this model, VSRs interact with their cargo in the ER, and the cargo-VSR complexes are transported from the ER to the TGN. Recycling of VSRs occurs at the TGN instead of the PVC. Subsequently, vacuolar cargoes are transported from the TGN to the PVC via maturation of the PVC from the TGN (Niemes et al., 2010b). However, multiple lines of extant evidence are inconsistent with this alternative model (daSilva et al., 2006; Foresti et al., 2010). In addition, this model brings many new questions. As suggested, if VSRs exit the ER in a COPII-independent manner, then which type of vesicle is involved in the ER export of VSRs? If they use clathrin-coated vesicles from the ER, then VSR Tyr mutants that may have a defect in interaction with adaptor protein complex should be retained in the ER. However, GFP-VSR2(Y612A) accumulates to the TGN and GFP-BP80-Y612A trafficked to the plasma membrane (daSilva et al., 2006; Foresti et al., 2010). Moreover, a vacuolar cargo Aleu-RFP was trapped in the ER when COPII-mediated ER export was inhibited by overexpression of Sec12 (Bottanelli et al., 2011). This alternative model was proposed based on the results of a study showing the localization of SNX2 at the TGN and redistribution of VSRs to the TGN in the presence of a mutant form of SNX (Niemes et al., 2010b). Therefore, there is a discrepancy between the localization of VSRs and sorting nexins in plants. This discrepancy might be caused by certain experimental conditions or the cell types used in these studies. In mammals, it has been suggested that the retromer complex functions as a coat protein as well as an adaptor complex for the recycling of sorting receptors, and unlike clathrin, the retromer complex remains associated with the recycling vesicles until the vesicles are tethered to the target membrane, indicating that it is possible that the retromer can localize to both donor and target membranes (McGough and Cullen, 2011). Consistent with this observation in animal cells, plant cells also appear to contain multiple complexes containing sorting nexin. Triple knockout sorting nexin mutant plants exhibit a defect only in the trafficking of 12S globulin, but *vps29* null mutant plants exhibit defects in the trafficking of both 12S globulin and 2S albumin, suggesting that the sorting nexin subcomplex and cargo-selective subcomplex do not always work together (Pourcher et al., 2010).

METHODS

Growth of Plants

Arabidopsis thaliana (ecotype Columbia-0 and the *mag1-1* mutant) (Shimada et al., 2006) was grown on B5 plates in a growth chamber at 20 to 22°C under a 16-h/8-h light/dark cycle. Leaf tissues from 2-week-old plants were used for protoplast isolation.

Construction of Plasmids

The *TPK1 cDNA* (At5g55630; NM_124945; Dunkel et al., 2008) was obtained by PCR using the specific primers TPK1-5 and TPK1-3. Primer sequences are given in Supplemental Table 1 online. The PCR product was digested with *Acc*65I and *Bam*HI and ligated into the downstream of the cauliflower mosaic virus (CaMV) 35S promoter in a vector with CaMV 35S promoter and YFP. The recycling defective *VSR1(L609A):myc* was generated by PCR-mediated site-directed mutagenesis using VSR1:myc as template (Kim et al., 2010). The first-round PCRs were performed using VSR1-XbaI-5/VSR1-L609A-SDM3 and VSR1-L609A-SDM5/NosT-End-ERI. Second-round PCR was performed using VSR1-XbaI-5/NosT-End-ERI primers using PCR products from first-round PCRs as template (see Supplemental Table 1 online). PCR product was digested with *Xba*I and *Eco*RI and ligated into the downstream of the CaMV 35S promoter in a vector. The sequence of all PCR products was verified by nucleotide sequencing.

Transient Expression and Immunoblot Analysis

Plasmids were introduced into protoplasts by polyethylene glycol–mediated transformation (Jin et al., 2001; Hyunjong et al., 2006). Transformed protoplasts were harvested at the appropriate time points after transformation and resuspended in sonication buffer (50 mM Tris-HCl, pH 7.5, 150 mM NaCl, 1 mM EDTA, 0.1% [v/v] Triton X-100, and protease inhibitor

cocktail [Roche Diagnostics]). Protoplasts were lysed by sonication, and the lysate was centrifuged at 5000*g* for 10 min to remove cellular debris. To prepare proteins from the culture medium, 100% (w/v) trichloroacetic acid (100 μL) was added to the medium (1 mL) and protein aggregates were precipitated by centrifugation at 10,000*g* at 4°C for 10 min. Protein aggregates were then dissolved in a solution of 0.1 N NaOH and analyzed by immunoblotting with anti-GFP (Bio-Application), anti-HA (Roche Diagnostics), anti-actin (MP Biomedicals), or anti-BiP (Lee et al., 2004a) antibodies, as described previously (Jin et al., 2001). Protein blots were developed with an ECL kit (Amersham Pharmacia Biotech), and images were obtained using a LAS3000 image capture system (FUJIFILM).

Immunofluorescence Staining and Microscopy

The expression of constructs was monitored at 24 HAT or indicated time points. Images of GFP, YFP, and mRFP fusion proteins were obtained in intact protoplasts in incubation medium on a glass slide covered with a cover slip. For immunostaining, transformed protoplasts were placed on poly-L-Lys–coated glass slides and incubated with 3% paraformaldehyde in fixing buffer (10 mM HEPES, pH 7.4, 154 mM NaCl, 125 mM $CaCl_2$, 2.5 mM maltose, and 5 mM KCl) for 1 h at room temperature (Park et al., 2005). The fixed cells were washed three times with TSW buffer (10 mM Tris-HCl, pH 7.4, 0.9% NaCl, 0.25% gelatin, 0.02% SDS, and 0.1% Triton X-100) and incubated with a rat monoclonal anti-HA or anti-myc (Cell Signaling Technology) or anti-SYP61 antibodies (Sanderfoot et al., 2001) at 4°C overnight. The protoplasts were then washed three times with TSW buffer and subsequently incubated with a tetramethylrhodamine-5-(and 6)-isothiocyanate (TRITC)–conjugated goat anti-rat IgG (Zymed), fluorescein isothiocyanate (FITC)–conjugated goat anti-rat IgG (Jackson ImmunoResearch Laboratories), Cy5-conjugated anti-rabbit IgG (Jackson ImmunoResearch Laboratories), or Alexa568 Donkey anti-mouse IgG (Molecular Probes) secondary antibodies. The immunostained protoplasts were mounted in medium (100 mM Tris-HCl, pH 8.5/25% glycerol) containing Mowiol4-88 (Calbiochem). Images were taken with a fluorescence microscope (Axioplan 2; Carl Zeiss) equipped with a ×40/0.75 objective (Plan-NEOFLUAR) and a cooled charge-coupled device camera (Senicam; PCO Imaging) at 20°C. The filter sets used were as follows: XF116 (exciter, 474AF20; dichroic, 500DRLP; emitter, 510AF23), XF33/E (exciter, 535DF35; dichroic, 570DRLP; emitter, 605DF50), and XF137 (exciter, 540AF30; dichroic, 570DRLP; emitter, 585ALP) (Omega) for GFP, mRFP, TRITC, and chlorophyll autofluorescence, respectively. For confocal laser scanning microscopy, fixed cells were examined with a Zeiss LSM 510 META laser scanning confocal microscope using objective C-APOCHROMAT X40/1.2W in the multitrack mode. Excitation/emission wavelengths were 488/505 to 530 nm for GFP, YFP, or FITC and 543/560 to 615 nm for TRITC. Transmitted light reference images were captured using differential interference contrast optics and argon laser illumination at 488 nm for GFP, YFP, and FITC or a HeNe laser at 543 nm for TRITC. The data were then processed using Adobe Photoshop software (Adobe Systems), and the images were rendered in pseudocolor (Jin et al., 2001; Kim et al., 2001).

Isolation of Total RNA and Quantitative RT-PCR Analysis of Transcript Levels

Total RNA was extracted from 1- or 2-week-old wild-type or *mag1-1* plants using an RNeasy plant mini kit (Qiagen) and digested with TURBO DNase (Ambion). Extracted RNA was reverse transcribed into cDNA using a High Capacity cDNA reverse transcription kit (Applied Biosystems). Quantitative real-time RT-PCR was performed with a SYBR green kit (Applied Biosystems) to detect *VSR1*, *VSR4*, *VSR5*, *VSR6*, *ACT8*, and *ACT2* transcripts. Amplified samples were normalized against *ACT8* and *ACT2* transcript levels (multiple internal controls). All primer pairs used are presented in Supplemental Table 1 online.

Accession Numbers

Sequence data from this article can be found in the Arabidopsis Genome Initiative or GenBank/EMBL databases under the following accession numbers: *Arabidopsis thaliana* TPK1, At5g55630; and At-VSR1, At3g52850.

Supplemental Data

The following materials are available in the online version of this article.

Supplemental Figure 1. Trafficking of TPK1:YFP to the Tonoplast Is Not Affected in *mag1-1* Plants.

Supplemental Figure 2. Overexpression of SYP21/PEP12p at Low Levels Does Not Compromise the Trafficking of Vacuolar Cargoes.

Supplemental Figure 3. Vacuolar Cargoes Do Not Accumulate to the Organelle to Which AtVSR1(L609A) Localizes in *mag1-1*.

Supplemental Figure 4. GFP:SYP61 Localizes to the SYP61-Positive Compartments.

Supplemental Table 1. Primers Used in This Study.

ACKNOWLEDGMENTS

This work was supported by grants from the National Research Foundation (NRF-20120001015), the World Class University Project (R31-2008-000-10105-0), the Advanced Biomass R&D Center (20110031340), the Ministry of Education, Science, and Technology (Korea), and grant from Ministry for Food, Agriculture, Forestry, and Fisheries (609004-05-4-SB240), Republic of Korea. E.J.S. was supported by a grant from the National Research Foundation (2011-0012880), and Y.L. was supported by a grant from the Next-Generation BioGreen 21 Program (PJ0080142011), Rural Development Administration, Republic of Korea.

AUTHOR CONTRIBUTIONS

H.K., I.H., and I.H.-N. conceived the project and designed the research strategies. H.K. conducted the majority of experiments. S.Y.K. carried out the real-time quantitative PCR. K.S. and D.W.L. performed localization of VSR1 with Spo:GFP. Y.L. generated the *TPK1:YFP* construct. E.J.S. generated GFP:SYP61. I.H. and H.K. wrote the article.

Received August 1, 2012; revised November 26, 2012; accepted December 6, 2012; published December 21, 2012.

REFERENCES

Ahmed, S.U., Bar-Peled, M., and Raikhel, N.V. (1997). Cloning and subcellular location of an *Arabidopsis* receptor-like protein that shares common features with protein-sorting receptors of eukaryotic cells. Plant Physiol. **114:** 325–336.

Arighi, C.N., Hartnell, L.M., Aguilar, R.C., Haft, C.R., and Bonifacino, J.S. (2004). Role of the mammalian retromer in sorting of the cation-independent mannose 6-phosphate receptor. J. Cell Biol. **165:** 123–133.

Bonifacino, J.S., and Rojas, R. (2006). Retrograde transport from endosomes to the trans-Golgi network. Nat. Rev. Mol. Cell Biol. **7:** 568–579.

Bottanelli, F., Foresti, O., Hanton, S., and Denecke, J. (2011). Vacuolar transport in tobacco leaf epidermis cells involves a single

route for soluble cargo and multiple routes for membrane cargo. Plant Cell **23:** 3007–3025.

Chehab, E.W., Patharkar, O.R., and Cushman, J.C. (2007). Isolation and characterization of a novel v-SNARE family protein that interacts with a calcium-dependent protein kinase from the common ice plant, *Mesembryanthemum crystallinum*. Planta **225:** 783–799.

Collins, B.M. (2008). The structure and function of the retromer protein complex. Traffic **9:** 1811–1822.

Crowley, K.S., Liao, S., Worrell, V.E., Reinhart, G.D., and Johnson, A.E. (1994). Secretory proteins move through the endoplasmic reticulum membrane via an aqueous, gated pore. Cell **78:** 461–471.

Cullen, P.J. (2008). Endosomal sorting and signalling: An emerging role for sorting nexins. Nat. Rev. Mol. Cell Biol. **9:** 574–582.

daSilva, L.L., Foresti, O., and Denecke, J. (2006). Targeting of the plant vacuolar sorting receptor BP80 is dependent on multiple sorting signals in the cytosolic tail. Plant Cell **18:** 1477–1497.

daSilva, L.L., Taylor, J.P., Hadlington, J.L., Hanton, S.L., Snowden, C.J., Fox, S.J., Foresti, O., Brandizzi, F., and Denecke, J. (2005). Receptor salvage from the prevacuolar compartment is essential for efficient vacuolar protein targeting. Plant Cell **17:** 132–148.

DeFalco, T.A., Bender, K.W., and Snedden, W.A. (2009). Breaking the code: Ca^{2+} sensors in plant signalling. Biochem. J. **425:** 27–40.

De Marcos Lousa, C., Gershlick, D.C., and Denecke, J. (2012). Mechanisms and concepts paving the way towards a complete transport cycle of plant vacuolar sorting receptors. Plant Cell **24:** 1714–1732.

Denecke, J., Aniento, F., Frigerio, L., Hawes, C., Hwang, I., Mathur, J., Neuhaus, J.M., and Robinson, D.G. (2012). Secretory pathway research: The more experimental systems the better. Plant Cell **24:** 1316–1326.

Dunkel, M., Latz, A., Schumacher, K., Müller, T., Becker, D., and Hedrich, R. (2008). Targeting of vacuolar membrane localized members of the TPK channel family. Mol. Plant **1:** 938–949.

Foresti, O., daSilva, L.L., and Denecke, J. (2006). Overexpression of the *Arabidopsis* syntaxin PEP12/SYP21 inhibits transport from the prevacuolar compartment to the lytic vacuole in vivo. Plant Cell **18:** 2275–2293.

Foresti, O., Gershlick, D.C., Bottanelli, F., Hummel, E., Hawes, C., and Denecke, J. (2010). A recycling-defective vacuolar sorting receptor reveals an intermediate compartment situated between prevacuoles and vacuoles in tobacco. Plant Cell **22:** 3992–4008.

Frigerio, L., de Virgilio, M., Prada, A., Faoro, F., and Vitale, A. (1998). Sorting of phaseolin to the vacuole is saturable and requires a short C-terminal peptide. Plant Cell **10:** 1031–1042.

Gabel, C.A., Goldberg, D.E., and Kornfeld, S. (1982). Lysosomal enzyme oligosaccharide phosphorylation in mouse lymphoma cells: Specificity and kinetics of binding to the mannose 6-phosphate receptor in vivo. J. Cell Biol. **95:** 536–542.

Harasaki, K., Lubben, N.B., Harbour, M., Taylor, M.J., and Robinson, M.S. (2005). Sorting of major cargo glycoproteins into clathrin-coated vesicles. Traffic **6:** 1014–1026.

Hwang, I. (2008). Sorting and anterograde trafficking at the Golgi apparatus. Plant Physiol. **148:** 673–683.

Hyunjong, B., Lee, D.S., and Hwang, I. (2006). Dual targeting of xylanase to chloroplasts and peroxisomes as a means to increase protein accumulation in plant cells. J. Exp. Bot. **57:** 161–169.

Jaillais, Y., Fobis-Loisy, I., Miège, C., Rollin, C., and Gaude, T. (2006). AtSNX1 defines an endosome for auxin-carrier trafficking in *Arabidopsis*. Nature **443:** 106–109.

Jaillais, Y., Santambrogio, M., Rozier, F., Fobis-Loisy, I., Miège, C., and Gaude, T. (2007). The retromer protein VPS29 links cell polarity and organ initiation in plants. Cell **130:** 1057–1070.

Jin, J.B., Kim, Y.A., Kim, S.J., Lee, S.H., Kim, D.H., Cheong, G.W., and Hwang, I. (2001). A new dynamin-like protein, ADL6, is involved in trafficking from the trans-Golgi network to the central vacuole in *Arabidopsis*. Plant Cell **13:** 1511–1526.

Jung, C., Lee, G.J., Jang, M., Lee, M., Lee, J., Kang, H., Sohn, E.J., and Hwang, I. (2011). Identification of sorting motifs of AtβFruct4 for trafficking from the ER to the vacuole through the Golgi and PVC. Traffic **12:** 1774–1792.

Jürgens, G. (2004). Membrane trafficking in plants. Annu. Rev. Cell Dev. Biol. **20:** 481–504.

Kim, H., Kang, H., Jang, M., Chang, J.H., Miao, Y., Jiang, L., and Hwang, I. (2010). Homomeric interaction of AtVSR1 is essential for its function as a vacuolar sorting receptor. Plant Physiol. **154:** 134–148.

Kim, H., Park, M., Kim, S.J., and Hwang, I. (2005). Actin filaments play a critical role in vacuolar trafficking at the Golgi complex in plant cells. Plant Cell **17:** 888–902.

Kim, Y.W., Park, D.S., Park, S.C., Kim, S.H., Cheong, G.W., and Hwang, I. (2001). *Arabidopsis* dynamin-like 2 that binds specifically to phosphatidylinositol 4-phosphate assembles into a high-molecular weight complex in vivo and in vitro. Plant Physiol. **127:** 1243–1255.

Kirsch, T., Paris, N., Butler, J.M., Beevers, L., and Rogers, J.C. (1994). Purification and initial characterization of a potential plant vacuolar targeting receptor. Proc. Natl. Acad. Sci. USA **91:** 3403–3407.

Kirsch, T., Saalbach, G., Raikhel, N.V., and Beevers, L. (1996). Interaction of a potential vacuolar targeting receptor with amino- and carboxyl-terminal targeting determinants. Plant Physiol. **111:** 469–474.

Lee, G.J., Kim, H., Kang, H., Jang, M., Lee, D.W., Lee, S., and Hwang, I. (2007). EpsinR2 interacts with clathrin, adaptor protein-3, AtVTI12, and phosphatidylinositol-3-phosphate. Implications for EpsinR2 function in protein trafficking in plant cells. Plant Physiol. **143:** 1561–1575.

Lee, G.J., Sohn, E.J., Lee, M.H., and Hwang, I. (2004a). The *Arabidopsis* rab5 homologs rha1 and ara7 localize to the prevacuolar compartment. Plant Cell Physiol. **45:** 1211–1220.

Lee, M.C., Miller, E.A., Goldberg, J., Orci, L., and Schekman, R. (2004b). Bi-directional protein transport between the ER and Golgi. Annu. Rev. Cell Dev. Biol. **20:** 87–123.

Lee, M.H., Jung, C., Lee, J., Kim, S.Y., Lee, Y., and Hwang, I. (2011). An *Arabidopsis* prenylated Rab acceptor 1 isoform, AtPRA1.B6, displays differential inhibitory effects on anterograde trafficking of proteins at the endoplasmic reticulum. Plant Physiol. **157:** 645–658.

Li, Y.B., Rogers, S.W., Tse, Y.C., Lo, S.W., Sun, S.S., Jauh, G.Y., and Jiang, L. (2002). BP-80 and homologs are concentrated on post-Golgi, probable lytic prevacuolar compartments. Plant Cell Physiol. **43:** 726–742.

Marcusson, E.G., Horazdovsky, B.F., Cereghino, J.L., Gharakhanian, E., and Emr, S.D. (1994). The sorting receptor for yeast vacuolar carboxypeptidase Y is encoded by the VPS10 gene. Cell **77:** 579–586.

Matsuoka, K., Bassham, D.C., Raikhel, N.V., and Nakamura, K. (1995). Different sensitivity to wortmannin of two vacuolar sorting signals indicates the presence of distinct sorting machineries in tobacco cells. J. Cell Biol. **130:** 1307–1318.

McGough, I.J., and Cullen, P.J. (2011). Recent advances in retromer biology. Traffic **12:** 963–971.

Miao, Y., Yan, P.K., Kim, H., Hwang, I., and Jiang, L. (2006). Localization of green fluorescent protein fusions with the seven *Arabidopsis* vacuolar sorting receptors to prevacuolar compartments in tobacco BY-2 cells. Plant Physiol. **142:** 945–962.

Niemes, S., Labs, M., Scheuring, D., Krueger, F., Langhans, M., Jesenofsky, B., Robinson, D.G., and Pimpl, P. (2010a). Sorting of plant vacuolar proteins is initiated in the ER. Plant J. **62:** 601–614.

Niemes, S., Langhans, M., Viotti, C., Scheuring, D., San Wan Yan, M., Jiang, L., Hillmer, S., Robinson, D.G., and Pimpl, P. (2010b). Retromer recycles vacuolar sorting receptors from the trans-Golgi network. Plant J. **61:** 107–121.

Nothwehr, S.F., Ha, S.A., and Bruinsma, P. (2000). Sorting of yeast membrane proteins into an endosome-to-Golgi pathway involves direct interaction of their cytosolic domains with Vps35p. J. Cell Biol. **151:** 297–310.

Oliviusson, P., Heinzerling, O., Hillmer, S., Hinz, G., Tse, Y.C., Jiang, L., and Robinson, D.G. (2006). Plant retromer, localized to the prevacuolar compartment and microvesicles in *Arabidopsis*, may interact with vacuolar sorting receptors. Plant Cell **18:** 1239–1252.

Paris, N., and Neuhaus, J.M. (2002). BP-80 as a vacuolar sorting receptor. Plant Mol. Biol. **50:** 903–914.

Park, M., Lee, D., Lee, G.J., and Hwang, I. (2005). AtRMR1 functions as a cargo receptor for protein trafficking to the protein storage vacuole. J. Cell Biol. **170:** 757–767.

Pfeffer, S.R. (2007). Unsolved mysteries in membrane traffic. Annu. Rev. Biochem. **76:** 629–645.

Pourcher, M., Santambrogio, M., Thazar, N., Thierry, A.M., Fobis-Loisy, I., Miège, C., Jaillais, Y., and Gaude, T. (2010). Analyses of sorting nexins reveal distinct retromer-subcomplex functions in development and protein sorting in *Arabidopsis thaliana*. Plant Cell **22:** 3980–3991.

Rapoport, T.A., Rolls, M.M., and Jungnickel, B. (1996). Approaching the mechanism of protein transport across the ER membrane. Curr. Opin. Cell Biol. **8:** 499–504.

Richter, S., Voss, U., and Jürgens, G. (2009). Post-Golgi traffic in plants. Traffic **10:** 819–828.

Robinson, D.G., Pimpl, P., Scheuring, D., Stierhof, Y.D., Sturm, S., and Viotti, C. (2012). Trying to make sense of retromer. Trends Plant Sci. **17:** 431–439.

Saint-Jean, B., Seveno-Carpentier, E., Alcon, C., Neuhaus, J.M., and Paris, N. (2010). The cytosolic tail dipeptide Ile-Met of the pea receptor BP80 is required for recycling from the prevacuole and for endocytosis. Plant Cell **22:** 2825–2837.

Sanderfoot, A.A., Ahmed, S.U., Marty-Mazars, D., Rapoport, I., Kirchhausen, T., Marty, F., and Raikhel, N.V. (1998). A putative vacuolar cargo receptor partially colocalizes with AtPEP12p on a prevacuolar compartment in *Arabidopsis* roots. Proc. Natl. Acad. Sci. USA **95:** 9920–9925.

Sanderfoot, A.A., Kovaleva, V., Bassham, D.C., and Raikhel, N.V. (2001). Interactions between syntaxins identify at least five SNARE complexes within the Golgi/prevacuolar system of the *Arabidopsis* cell. Mol. Biol. Cell **12:** 3733–3743.

Seaman, M.N. (2004). Cargo-selective endosomal sorting for retrieval to the Golgi requires retromer. J. Cell Biol. **165:** 111–122.

Seaman, M.N., Marcusson, E.G., Cereghino, J.L., and Emr, S.D. (1997). Endosome to Golgi retrieval of the vacuolar protein sorting receptor, Vps10p, requires the function of the VPS29, VPS30, and VPS35 gene products. J. Cell Biol. **137:** 79–92.

Seaman, M.N., McCaffery, J.M., and Emr, S.D. (1998). A membrane coat complex essential for endosome-to-Golgi retrograde transport in yeast. J. Cell Biol. **142:** 665–681.

Shimada, T., Fuji, K., Tamura, K., Kondo, M., Nishimura, M., and Hara-Nishimura, I. (2003). Vacuolar sorting receptor for seed storage proteins in *Arabidopsis thaliana*. Proc. Natl. Acad. Sci. USA **100:** 16095–16100.

Shimada, T., Koumoto, Y., Li, L., Yamazaki, M., Kondo, M., Nishimura, M., and Hara-Nishimura, I. (2006). AtVPS29, a putative component of a retromer complex, is required for the efficient sorting of seed storage proteins. Plant Cell Physiol. **47:** 1187–1194.

Sohn, E.J., Kim, E.S., Zhao, M., Kim, S.J., Kim, H., Kim, Y.W., Lee, Y.J., Hillmer, S., Sohn, U., Jiang, L., and Hwang, I. (2003). Rha1, an *Arabidopsis* Rab5 homolog, plays a critical role in the vacuolar trafficking of soluble cargo proteins. Plant Cell **15:** 1057–1070.

Song, J., Lee, M.H., Lee, G.J., Yoo, C.M., and Hwang, I. (2006). *Arabidopsis* EPSIN1 plays an important role in vacuolar trafficking of soluble cargo proteins in plant cells via interactions with clathrin, AP-1, VTI11, and VSR1. Plant Cell **18:** 2258–2274.

Tamura, K., Shimada, T., Kondo, M., Nishimura, M., and Hara-Nishimura, I. (2005). KATAMARI1/MURUS3 Is a novel golgi membrane protein that is required for endomembrane organization in *Arabidopsis*. Plant Cell **17:** 1764–1776.

Tamura, K., Shimada, T., Ono, E., Tanaka, Y., Nagatani, A., Higashi, S.I., Watanabe, M., Nishimura, M., and Hara-Nishimura, I. (2003). Why green fluorescent fusion proteins have not been observed in the vacuoles of higher plants. Plant J. **35:** 545–555.

Tang, B.L., Wang, Y., Ong, Y.S., and Hong, W. (2005). COPII and exit from the endoplasmic reticulum. Biochim. Biophys. Acta **1744:** 293–303.

Traub, L.M. (2005). Common principles in clathrin-mediated sorting at the Golgi and the plasma membrane. Biochim. Biophys. Acta **1744:** 415–437.

Tse, Y.C., Mo, B., Hillmer, S., Zhao, M., Lo, S.W., Robinson, D.G., and Jiang, L. (2004). Identification of multivesicular bodies as prevacuolar compartments in *Nicotiana tabacum* BY-2 cells. Plant Cell **16:** 672–693.

Uemura, T., Ueda, T., Ohniwa, R.L., Nakano, A., Takeyasu, K., and Sato, M.H. (2004). Systematic analysis of SNARE molecules in *Arabidopsis*: Dissection of the post-Golgi network in plant cells. Cell Struct. Funct. **29:** 49–65.

Vitale, A., and Raikhel, N.V. (1999). What do proteins need to reach different vacuoles? Trends Plant Sci. **4:** 149–155.

Zouhar, J., Muñoz, A., and Rojo, E. (2010). Functional specialization within the vacuolar sorting receptor family: VSR1, VSR3 and VSR4 sort vacuolar storage cargo in seeds and vegetative tissues. Plant J. **64:** 577–588.